AD_____

Award Number: W81XWH-04-1-0827

TITLE: Potentiation of Prostate Cancer Radiotherapy Using Combined Antiangiogenic and Antitumor Therapies

PRINCIPAL INVESTIGATOR: Bruce M. Fenton, Ph.D.

CONTRACTING ORGANIZATION: University of Rochester
Rochester, NY 14642

REPORT DATE: October 2005

TYPE OF REPORT: Annual

PREPARED FOR: U.S. Army Medical Research and Materiel Command
Fort Detrick, Maryland 21702-5012

DISTRIBUTION STATEMENT: Approved for Public Release;
Distribution Unlimited

20060503174

REPORT DOCUMENTATION PAGE		*Form Approved* OMB No. 0704-0188

Public reporting burden for this collection of information is estimated to average 1 hour per response, including the time for reviewing instructions, searching existing data sources, gathering and maintaining the data needed, and completing and reviewing this collection of information. Send comments regarding this burden estimate or any other aspect of this collection of information, including suggestions for reducing this burden to Department of Defense, Washington Headquarters Services, Directorate for Information Operations and Reports (0704-0188), 1215 Jefferson Davis Highway, Suite 1204, Arlington, VA 22202-4302. Respondents should be aware that notwithstanding any other provision of law, no person shall be subject to any penalty for failing to comply with a collection of information if it does not display a currently valid OMB control number. **PLEASE DO NOT RETURN YOUR FORM TO THE ABOVE ADDRESS.**

1. REPORT DATE 01-10-2005	2. REPORT TYPE Annual	3. DATES COVERED 10 Sep 2004 – 9 Sep 2005
4. TITLE AND SUBTITLE Potentiation of Prostate Cancer Radiotherapy Using Combined Antiangiogenic and Antitumor Therapies		5a. CONTRACT NUMBER
		5b. GRANT NUMBER W81XWH-04-1-0827
		5c. PROGRAM ELEMENT NUMBER
6. AUTHOR(S) Bruce M. Fenton, Ph.D.		5d. PROJECT NUMBER
		5e. TASK NUMBER
		5f. WORK UNIT NUMBER
7. PERFORMING ORGANIZATION NAME(S) AND ADDRESS(ES) University of Rochester Rochester, NY 14642		8. PERFORMING ORGANIZATION REPORT NUMBER
9. SPONSORING / MONITORING AGENCY NAME(S) AND ADDRESS(ES) U.S. Army Medical Research and Materiel Command Fort Detrick, Maryland 21702-5012		10. SPONSOR/MONITOR'S ACRONYM(S)
		11. SPONSOR/MONITOR'S REPORT NUMBER(S)

12. DISTRIBUTION / AVAILABILITY STATEMENT
Approved for Public Release; Distribution Unlimited

13. SUPPLEMENTARY NOTES

14. ABSTRACT
The purpose of this phase of the grant was to quantitate response to antiangiogenic and radiation therapy, in terms of changes in tumor vascular function and hypoxia, and to use the pathophysiological findings to optimally schedule combined therapies. Following a variety of treatments, ~250 tumors were frozen for immunohistochemical staining and image analysis (and stored for future molecular assays). Methods were developed for colocalized staining of a panel of pericyte markers, apoptosis, total/perfused vessels, hypoxia, and necrosis. A multiple receptor inhibitor, AG-013736, was shown to provide striking tumor response in the absence of marked pathophysiological alterations. Initial findings indicate that combining this drug with radiation may reduce some of the tumor volume-dependent resistance seen in single agent therapy. Ongoing studies will quantitate treatment-induced alterations in pericyte coverage in the initial DU145 prostate tumors, as well as PC-3 and MDA-PDa-2b tumor models.

15. SUBJECT TERMS
Angiogenesis, tumor vasculature, hypoxia, tumor pthophysiology

16. SECURITY CLASSIFICATION OF:			17. LIMITATION OF ABSTRACT	18. NUMBER OF PAGES	19a. NAME OF RESPONSIBLE PERSON USAMRMC
a. REPORT U	b. ABSTRACT U	c. THIS PAGE U	UU	15	19b. TELEPHONE NUMBER *(include area code)*

Standard Form 298 (Rev. 8-98)
Prescribed by ANSI Std. Z39.18

Table of Contents

Introduction:

Although radiation therapy (RT) has been shown effective for localized prostate cancer, failures continue to occur at high rates. Recognizing that the tumor is comprised of distinct cellular compartments under heterogeneous microenvironmental conditions, we are investigating a unique and innovative combination of specifically targeted therapies: 1) Conventional fractionated RT is used to sterilize oxygenated tumor cells. 2) Specific inhibitors of several angiogenic growth factor receptors target both mature and newly formed blood vessels, halting tumor expansion by blocking the hypoxia-induced overexpression of angiogenic cytokines and potentiating RT by sensitizing the tumor vasculature to radiation-induced apoptosis. 3) Finally, blockers of IGF-IR, which is overexpressed in prostate tumors, sensitize the hypoxic compartment of the tumor, which would otherwise be relatively radioresistant. Unfortunately, both RT and antiangiogenic strategies can in themselves lead to increased hypoxia, not only compromising further RT but also possibly increasing the risk of metastatic disease. To gauge the overall effects of our combined therapies on tumor oxygenation heterogeneities, as well as to determine whether our strategies are targeting the intended tumor and endothelial cell compartments, we are quantifying the underlying microregional pathophysiological and molecular changes using: 1) automated methods for immunohistochemical image acquisition across entire tumor frozen sections, 2) image overlay techniques for revisiting the same locations following consecutive staining protocols with contrasting fluorochromes, and 3) image analysis macros for spatially characterizing hypoxia, apoptosis, and proliferation as a function of distance from total or perfused blood vessels. Initial studies have clearly demonstrated that the effects of combination therapies are not simply the sum of the individual effects when it comes to pathophysiological alterations. Whereas either antiangiogenic strategies or RT can induce hypoxia, the combination can sometimes improve tumor oxygenation.

Body:

During this first year of our studies, a major focus has been in establishing and optimizing the new immunohistochemical staining and image analysis techniques required in Tasks 1 and 2 for quantifying tumor vascular function and endothelial damage. Methods for determining tumor hypoxia in relation to total and perfused blood vessel distributions were already in place and have been applied to the new tumor models. In addition, immunohistochemical protocols were (and continue to be) developed and optimized for combined fluorescent staining of combinations of vessel markers (Panec, CD31), pericyte and smooth muscle markers (α-sma, desmin, NG2, and PDGFR-β), apoptosis, and activated VEGFR-2.

Since the growth of the human xenografts is a fairly time-consuming process (requiring 6 wks from in vitro propagation to the formation of ~100 mm^3 tumors), parallel studies were initiated to investigate the response of the tumors to radiation, antiangiogenic agents, and combination therapies, while at the same time optimizing the immunohistochemical staining. Since all tumors are frozen and stored at -80°C following treatment, the samples remain available for cryostat sectioning as well as molecular

assays once the optimal staining protocols are finalized. These studies will be continued in Year 2.

Tumor Models:
Year 1 studies began with the in vitro and in vivo establishment of both the PC-3 and DU145 human prostate xenograft tumor models, neither of which we had previously worked with. The majority of the initial radiation and antiangiogenic studies in this report were thus far carried out with only the DU145.

Antiangiogenic and antitumor treatments:
As was detailed in the initial grant application, we foresaw that the specific antiangiogenic agents to be included in Tasks 2 and 3 might vary, depending on the most promising investigational antibodies available at the time experiments were initiated. In the application, we proposed to include several ImClone Systems antibodies: a) DC101 (anti-VEGFR-2), b) A12 (anti-IGF-1R), and c) C225 (anti-EGFR), and our initial experiments with the DU145 tumors were performed with the DC101 and A12 in combination with fractionated RT. Over the past year, however, we also finalized a Material Transfer Agreement with Pfizer Global Research to provide two promising small molecule tyrosine kinase inhibitors: a) AG-028262, a blocker of VEGFR-1,2,3, and b) AG-013736, a blocker of VEGFR-1,2,3 as well as PDGFR-b, FGFR, and c-kit. As we have been trying to obtain these multiple receptor blockers for quite some time, and also in view of the somewhat marginal response of the DU145 tumors to A12, we switched our focus at this time to concentrate on combinations of RT with these small molecule inhibitors.

Tumor response to A12, DC101, RT, and combination therapies:
Our first tumor response experiments looked at the effects of fractionated RT, DC101, and A12 alone on tumor growth progression. In two consecutive experiments, DU145 tumors were implanted in 100 male nu/nu mice, grown to ~250 mm^3, and treatment was administered for 3 wks (45 mg/kg every other day, i.p. for the A12 and DC101, 2 Gy $\times$ 5 day/wk for the RT). As shown in Fig. 1A, all treatments significantly delayed tumor growth, A12 producing the least effect and DC101, the most striking. The addition of the anti-IGF-1R (A12) to either RT or DC101 had no substantial effect on tumor growth, as shown in Fig. 1B.

For these mice, EF5 was injected i.v. 1 hr prior to tumor freezing (to quantify tumor hypoxia distributions) and DiOC$_7$ was injected 1 min prior to freezing (to delineate perfused tumor blood vessels). Following tumor sectioning, anti-panendothelial antigen (Panec) staining was also utilized to mark total blood vessel spacing. Using image analysis techniques[1], mean distances to the nearest perfused or total blood vessel were determined as shown in Fig. 2. These measures provide an estimate of the distribution of distances required for oxygen and nutrients to diffuse to all cell in the tumor, and are presented in relation to both total anatomical blood vessels and functionally perfused vessels. As seen in the figure, both DC101 alone and the combination of DC101 + A12 resulted in significantly increased vascular spacing (corresponding to reduced vessel densities). RT or A12 alone, however, had no substantial effect. Overall EF5 intensities

5

(an i.v. injected nitroimidazole compound that binds to hypoxic cells and is recognized by a fluorescently conjugated antibody in the frozen sections) were also determined, as shown in Fig. 3. As will be further discussed later, DU145 tumors appear fairly well vascularized and oxygenated to begin with, and although both DC101 and the combination reduced perfused vessel counts, hypoxia was only slightly elevated, even in the case of the combination treatment.

Tumor response to AG-028262, AG-013736, RT, and combinations:
Preliminary experiments were performed with the AG-028262 to gauge the dependence on drug dose. Three doses (5, 20, or 80 mg/kg) were administered daily by gavage, beginning at volumes of 150-200 mm^3, and tumor growth was recorded. Since this was our first experience in drug administration by gavage, actual ingested doses are somewhat suspect, but a clear response to the drug was evident at the 80 mg/kg dose. By the end of this experiment, we were confident in our ability to gavage the animals, and an additional experiment was performed at 40 mg/kg, at a somewhat larger treatment initiation tumor volume to ensure that tumor growth suppression was achieved, without total regression. This ensured that synergistic or additive effects of the RT combinations to follow would
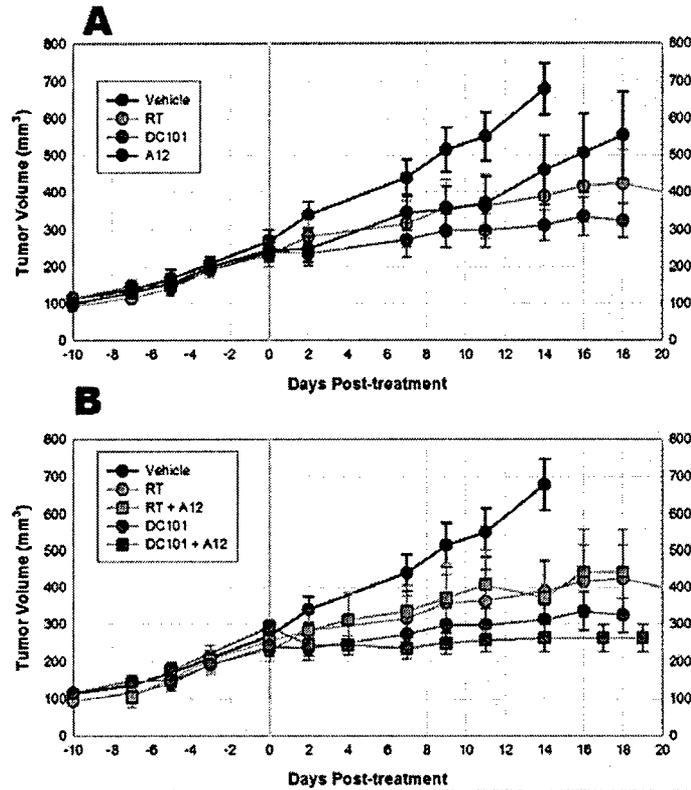
Figure 1

Fig. 1 – A) DU145 tumor growth following fractionated radiation (RT), DC101, or A12. Yellow line marks treatment start date. B) Response to combined therapies.

Figure 2
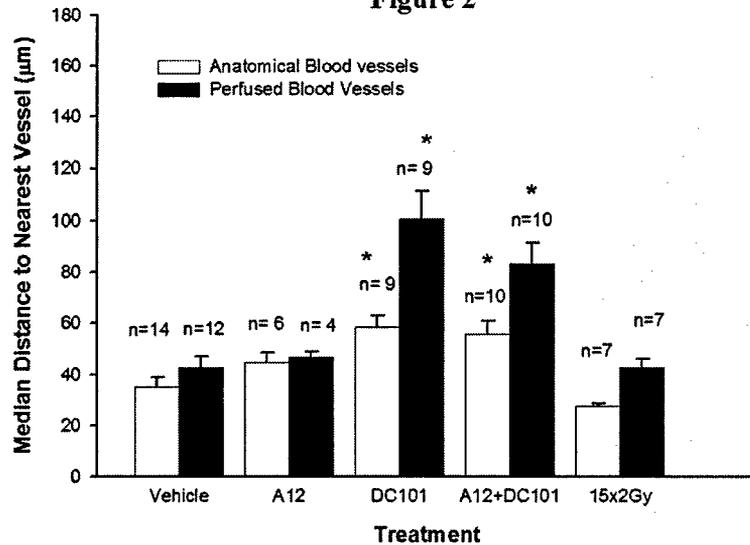
Fig. 2 – Total (open bars) versus perfused (filled bars) vessel spacing. N = number of tumors per group. * = p < 0.05 versus controls.

be readily apparent. A preliminary analysis of total and perfused vessel spacing was also completed for the 40 mg/kg treatments, and it was found that both total and perfused vessel spacings increased significantly in relation to controls (p = 0.05 and p = 0.02, respectively). Hypoxia, as determined by overall EF5 intensities, was unchanged.
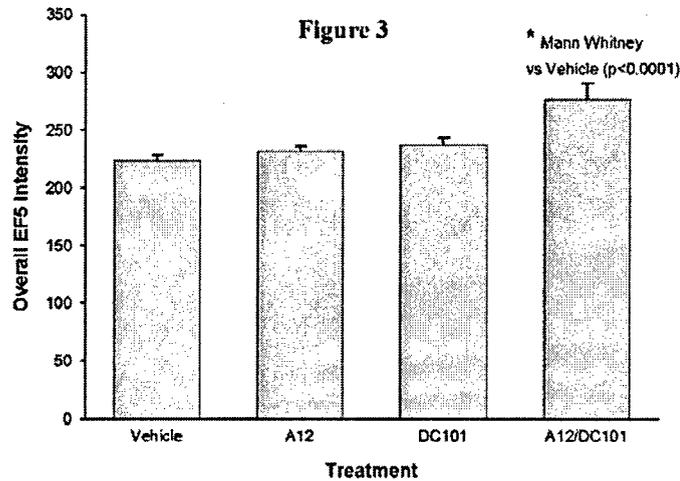
Fig. 3 – Changes in overall hypoxia with treatment.

Based on these preliminary results, a somewhat more comprehensive experiment was carried out to obtain a quick sense of whether or not the sequence of combination therapies would significantly alter tumor response. Here the hypothesis was that tumors in which oxygenation is compromised by the antiangiogenic therapy will be more resistant to subsequent RT, and RT may be more effective if administered prior to the antiangiogenic. Fig. 4 summarizes the growth response to 6 different treatments which continued for 2 weeks: 1) vehicle alone, 2) AG-028262 alone (40 mg/kg), 3) RT alone (5 × 2 Gy/wk, 4) 1 wk RT, then RT+AG, 5) 1 wk AG, then RT+AG, and 6) 2 wk concurrent RT+AG. Since the major purpose of these experiments was to gauge growth delay, treatment was only administered for 2 wks, at which time tumors were allowed to recover for up to another 3 wks.

Figure 4
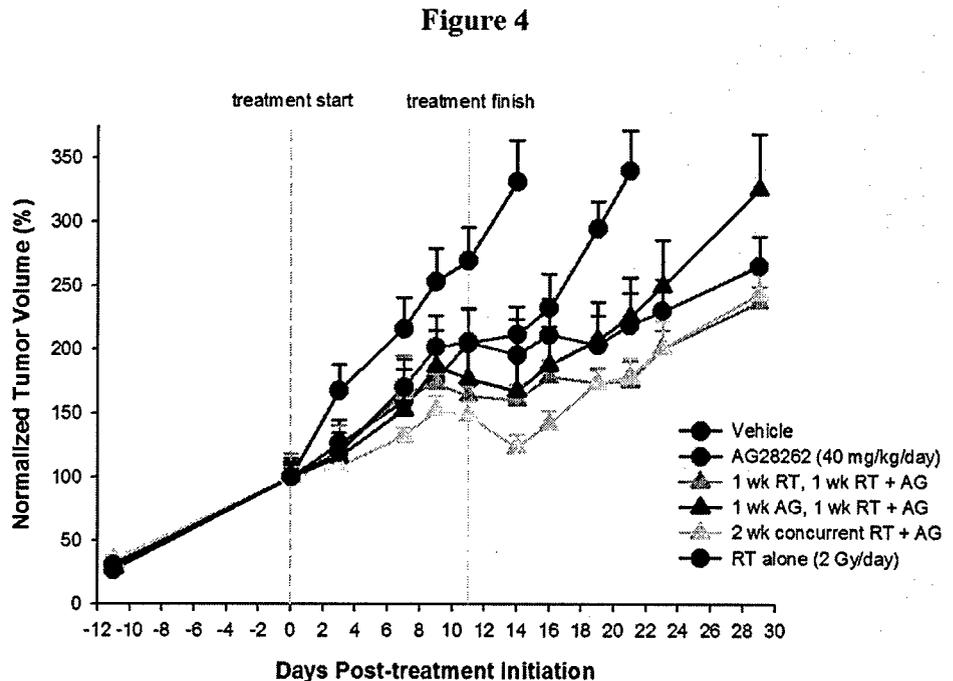
Fig. 4 – Effect of treatment scheduling on DU145 tumor growth. AG-028262 administered pre-, post-, or concurrently with RT.

Figure 5
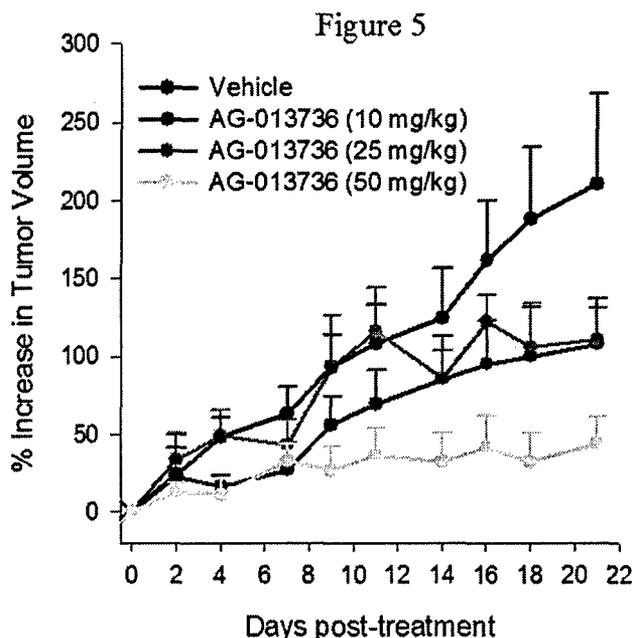
Fig. 5 – Dose response curves for AG-013736 in DU145 tumors.

Figure 6
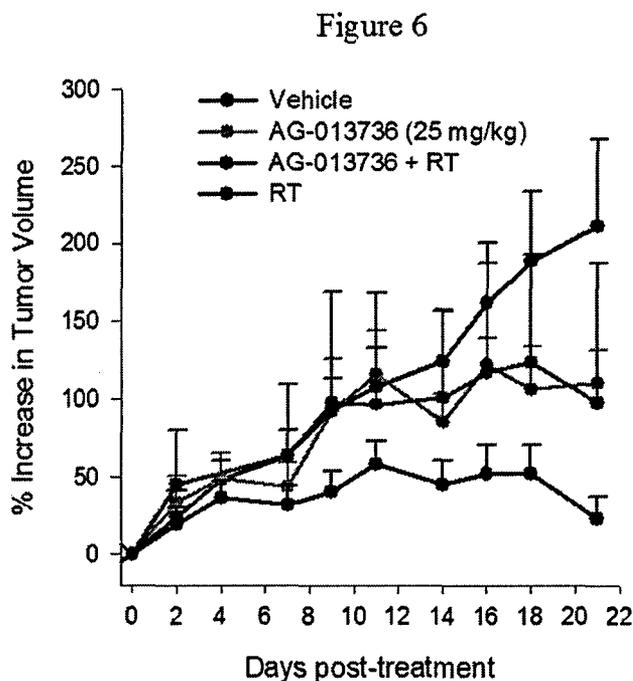
Fig. 6 – Effect of AG-013736 and RT on DU145 tumor growth.

At 40 mg/kg/day (red circles), the AG-028262 significantly inhibited tumor growth, somewhat equivalently to the fractionated radiation alone (2 Gy × 5/wk, pink symbols). After completion of treatment, however, the AG-028262 tumors grew at an increased rate in comparison to the RT tumors. Only the concurrent combination resulted in a temporary regression in tumor volume, immediately following treatment, but by 18 days post-treatment, tumor volumes were not significantly different between any of the combination treatments or radiation alone.

About 3 months ago, we obtained the first AG-013736 from Pfizer. Figure 5 shows the response of the DU145 tumors to three different doses of AG-013736 (10, 25, and 50 mg/kg/day). 10 and 25 mg/kg were somewhat similar, while 50 mg/kg produced almost a total cessation of tumor growth.

The dose of 25 mg/kg was next combined with fractionated radiation, as shown in Figure 6. Here RT or AG-013736 alone resulted in comparable growth inhibition, while the combination almost totally blocked tumor growth. [For Figures 5 and 6, treatments were initiated at tumor volumes of ~200-300 mm³].

An interesting aspect of these results was the response of the DU145 tumors to radiation alone. When growth curves for

8

individual tumors were plotted (Figure 7), it was noted that response was highly variable among tumors (as also shown by the large standard errors for the RT group in Figure 6). Individual tumor response to RT appeared to depend strongly on tumor volume at treatment initiation. Most tumors in which treatment was begun at volumes of < 300 mm^3, grew slowly if at all, while tumors treated at >300 mm^3 were fairly resistant to RT.

Figure 7
RT only - individual tumors
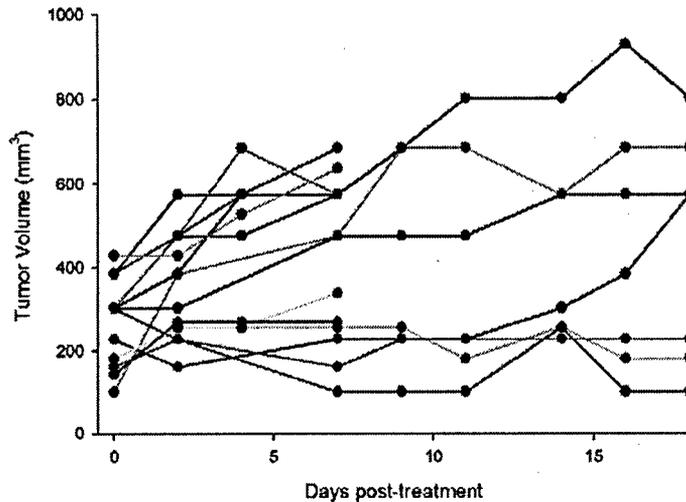
Fig. 7 – Response of individual DU145 tumors to RT. Note decreased response at larger treatment initiation volumes.

With the combination treatment (Figure 8 presents individual tumor data), all tumors remained fairly dormant throughout the three weeks of therapy, regardless of tumor initiation volume (4 of the 7 tumors were >300 mm^3). These results are highly intriguing and warrant further molecular and pathophysiological measurements to determine which factors may contribute to the variable radiosensitivity and how the AG-013736 may be affecting this radioresistance.

Figure 8
RT/AG-013736 - individual tumors
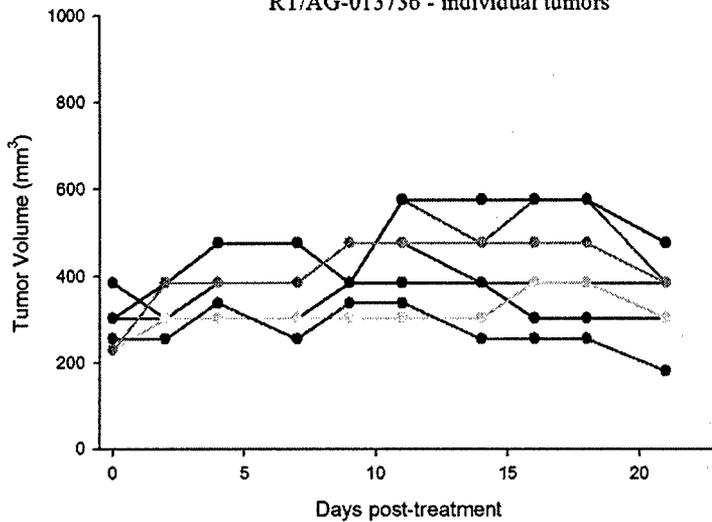
Fig. 8 – Response of individual DU145 tumors to AG-013736 (25 mg/kg).

Finally, we also looked at the initial response curves to AG-013736 in MCa-4 murine carcinomas (Figure 9). Treatment was initiated at 300 mm^3, and although we expected some growth inhibition, tumors grew at essentially the same rate as controls for each of the three doses: 10, 25, and 50 mg/kg/day. The reason for the lack of response in the murine tumors is unclear at this point.

9

Figure 9
MCa-4 Tumors
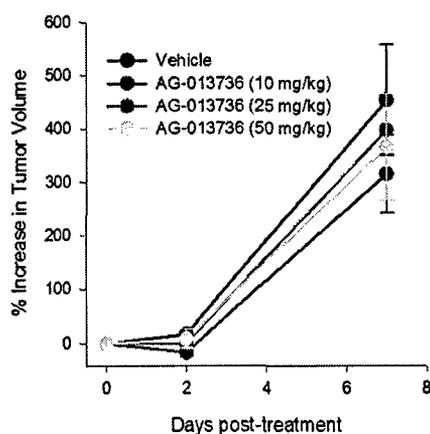
Figure 10

Fig. 9 – dose response curve for AG-013736 in MCa-4 mammary tumors	Fig. 10 – Changes in total (blue) and perfused (red) vessel spacing following treatment. * = p < 0.05 versus controls
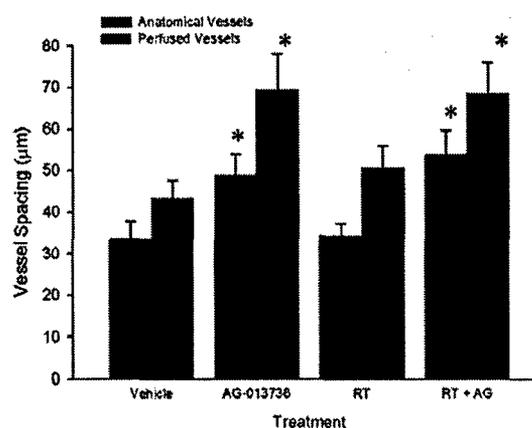
We are quite excited about continuing the studies with the AG-013736, in particular expanding to the PC-3 prostate tumor model. Our initial immunohistochemistry studies will look at total and perfused vessel spacing, tumor hypoxia, and various pericyte markers (smooth muscle actin, desmin, anti-PDGFR, and NG2, all colocalized with our perfused and total vessel markers).

Fig. 10 presents the initial pathophysiological data for the AG-013736 experiments. Somewhat similar to the AG-028262 experiments, either AG-013736 or the combination of RT + AG-013736 resulted in significant increases in both total and perfused vessel spacing, i.ndicating a pronounced inhibitory effect on vessel growth. Despite this, vascular densities remain quite high in this tumor even after treatment, in relation to previous tumor models (MCa-35 and MCa-4 mammary tumors, KHT sarcomas, as well as OW-1 and MLS ovarian xenografts), indicating that oxygenation may also be maintained. Fig. 11 presents the corresponding overall intensities. Although hypoxia is significantly increased in the combination treated tumors, the increase is not substantial in absolute terms. Since hypoxia levels did not increase with increasing distance from the blood vessels, the reduction in perfused vessels in probably not enough to compromise oxygen delivery following these single and combination treatments.

Immunohistochemical Staining Advances:
To more fully understand the underlying molecular mechanisms involved with the observed pathophysiological changes in these tumor lines, a number of additional immunohistochemical staining techniques have been incorporated and optimized over the first year. These focused particularly on identifying vascular pericytes and smooth muscle cells, as indicators of both vessel maturity and vascular "normalization", as outlined in Task 1. A wide range of pericyte markers have been reported in the literature, i.e., desmin, NG2, PDGFR, and α-sma, but it is widely accepted that no single marker is

10

definitive in all cases[2-4]. A second objective in the immunohistochemical studies was to establish dual and triple labeling protocols, such that pericyte coverage could be evaluated in relation to either perfused or anatomical blood vessels using alternate fluorescent colors. Finally, colocalization techniques were designed to combine overall TUNEL staining with various endothelial cell markers to quantitate endothelial as well as tumor cell apoptosis.

Immunohistochemical staining protocols for the following antibodies were optimized over the course of the past year both individually and in combination: apoptosis TUNEL assay plus CD31 vessel marker, pan-endothelial cell antigen (Panec) vessel marker plus alpha smooth muscle actin (α-sma), Panec plus desmin, α-sma plus desmin, activated VEGFR2 (p-VEGFR2) plus Panec, and p-VEGFR2 plus EF5 hypoxic marker. Optimization included testing different secondary antibody detection systems including chromagen based reagents, Cy3 and AlexaFluor 488/546 conjugated fluorescent antibodies for optimal multi-color labeling and to maximally differentiate positive signals for image analysis. Additionally, differences in section thickness were tested for optimum pericyte staining testing: 9, 20, 50, and 80 um thick sections.

Fig. 11 – Changes in overall hypoxia following treatment.

Pericyte markers:
Fig. 12 illustrates overlays of three alternative pericyte markers on Panec vessel staining (blue) and DiOC7 perfused vessel staining (green). Fig. 12A overlays PDGFR staining, 12B is NG2, and 12C is α-sma, all shown in red in serial frozen sections from the same DU145 tumor. The upper portion of the figures is the tumor tissue (implanted in the hind legs), and the multi-colored bands across the lower right corner are the adjoining muscle tissue. As can be seen in Fig. 12A, the muscle tissue is highly vascularized, with extensive overlap between the Panec and PDGFR (magenta), while the tumor tissue has little PDGFR associated with the vessels. In Fig. 12B, in contrast, the normal tissue has reduced NG2 staining, which has been reported to preferentially stain less mature pericytes[2], while the tumor tissue has extensive non-vessel associated staining. Finally Fig. 12C shows some overlap between the α-sma (presumably a marker of more mature pericytes / smooth muscle cells) and vessel staining in the muscle, but little tumor-associated pericyte staining. We have just acquired the first of our multi-stained images and are now beginning the implementation of image analysis methods for quantitating pericyte / endothelial overlap among the various treatment groups. In addition, thicker sections are also being cut to improve resolution of the endothelial marker in these tumors.

Fig. 12 – Panec endothelial staining (blue) and DiOC7 perfusion staining (green) superimposed on A) PDGFR (red), B) NG2 (red), or C) alpha-sma (red) for an untreated DU145 tumor.
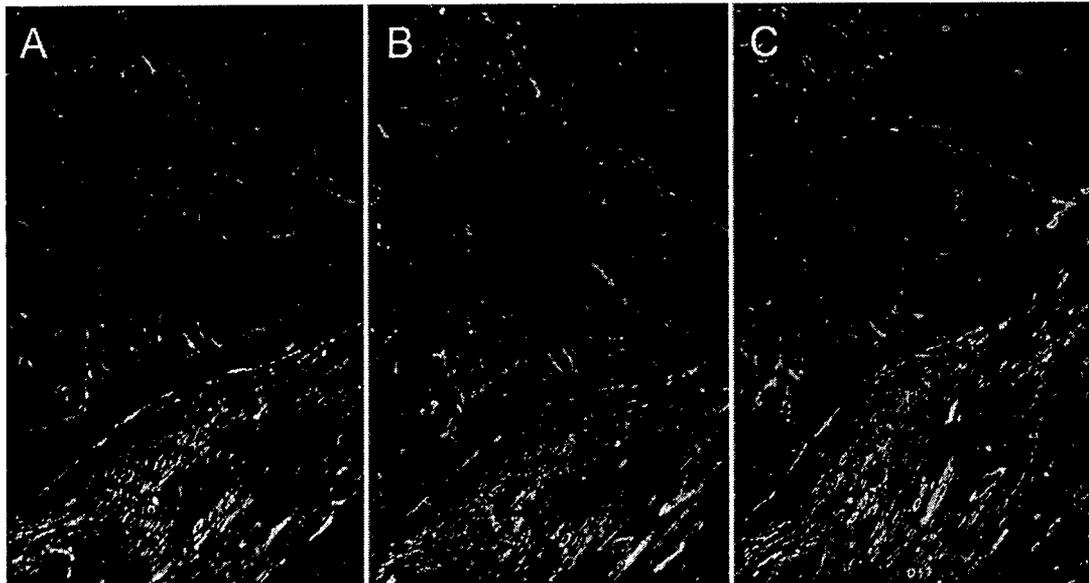
Key Research Accomplishments:

1) Intramuscular implantations of DU145 and PC-3 human prostate tumor models have been initiated and, thus far, 250 human xenograft tumors have been frozen following a range of treatment combinations, including intravascular injection of both the $DiOC_7$ perfusion marker and the EF5 hypoxic marker.
2) Tumor dose response curves were obtained for both AG-028262 and AG-013736.
3) Tumor growth curves were also obtained in respect to the following treatments and combinations (for the DU145 tumors):
   a. Vehicle alone (RT pr drug controls for each experiment)
   b. Fractionated RT (5 × 2 Gy/ wk × 3 wks)
   c. A12 (anti-IGF-1R)
   d. DC101 (anti-VEGFR-2)
   e. A12 + DC101
   f. A12 + RT
   g. AG-028262 (inhibitor of VEGFR-1,2,3)
   h. AG-013736 (inhibitor of VEGFR-1,2,3, PDGFRb, bFGF, and c-kit)
   i. AG-028262 + RT
   j. AG-013736 + RT
4) For the AG-028262, growth curves were also determined in response to three alternative treatment schedules: 1) AG for 1 wk followed by RT + AG for 1 wk, 2) RT for 1 wk followed by RT+ AG for 1 wk, and 3) RT + AG given concurrently for 2 wks.

5) Although A12 inhibited tumor growth somewhat similarly to fractionated RT, DC101 was more effective than either and was not markedly improved by the addition of A12.

6) Comparing RT and AG-028262 treatment schedules, concurrent therapy was the only combination that resulted in even temporary tumor regression. By 2 wks following treatment cessation, all 3 schedules were essentially equivalent in terms of tumor progression.

7) Tumor pathophysiological measures of total/perfused vessel spacing and hypoxia were also determined using immunohistochemistry and image analysis for most treatment combinations. AG-013736 essentially stopped tumor progression at a dose of 50 mg/kg. When combined with RT at a lower dose of 25 mg/kg, the combination appears to reduce some of the variable response seen with different stage tumors to RT alone. Despite the fact that AG-013736 substantially reduced total and perfused vessel counts, tumor hypoxia was not substantially increased, suggesting that in combination this agent will not compromise RT response.

8) A wide variety of new immunohistochemical staining procedures were implemented and optimized, including: 1) PDGFR, 2) α-sma, 3) desmin, 4) NG2, activated VEGFR-2, all colocalized with both $DiOC_7$ perfusion staining and Panec total vessel staining. Preliminary qualitative comparisons were made of controls, AG-013736, RT, and combination treated tumors in terms of colocalization between endothelial and pericyte staining, and quantitative assays are in progress.

Reportable Outcomes:

Abstracts and Presentations:

1) 2005 Radiation Research Meeting, Denver, CO. Pathophysiological effects of antibodies to IGF-1R and VEGFR-2 plus fractionated radiation in DU145 prostate carcinoma xenografts. BM Fenton and SF Paoni.

Conclusions:

In summary, the first year of this grant has concentrated on establishing the groundwork for the experiments to follow over the next two years and in acquiring frozen tumors for the immunohistochemical staining and imaging. Thus far, we have: 1) established and optimized six new immunohistochemical dual-staining protocols, 2) introduced two new human xenograft tumor models, 3) determined tumor growth response in DU145 tumors to a wide range of antiangiogenic and RT treatment monotherapies and combinations and frozen ~250 tumors for upcoming molecular evaluations.

We are most excited by our results using the combination of AG-013736 and fractionated RT, which in initial experiments produced almost a complete cessation or even regression in tumor growth in the DU145 tumors. We will next compare alternative scheduling of the antiangiogenic and RT therapies to determine whether RT may be more effective if delivered prior to the AG-013736 induced reduction in tumor perfused vessel counts. Since hypoxia was not markedly increased in the DU145 following AG-013736,

however, scheduling may be less important in this particular model. In Year 2, similar experiments will be repeated with both the PC-3 and MDA-PCa-2b tumor models.

Another intriguing aspect of the first years studies was the marked differences in response over a relatively small range of treatment initiation tumor volumes. Although response to RT varied widely when comparing 200 mm^3 to 400 mm^3 tumors, preliminary results showed much less dependence on tumor volume for the AG-013736 treatments. Further studies will expand on these results as well as determine whether the combination therapy is superior over this volume range.

The major focus of next year's work will be to build on this initial tumor database. Specifically, we will compare and correlate our newly developed staining procedures on multiple sections from the previously frozen tumors to gain a better understanding of the underlying mechanistic alterations that lead to the observed pathophysiological changes. Future work will: 1) develop and automate image analysis macros to quantitate the overlap between the pericyte and endothelial stains, 2) acquire additional timepoints for the RT studies, 3) look at angiogenic/antiangiogenic cytokine changes in the previously frozen tumors from Year 1 using gene arrays, 4) optimize scheduling of the AG-013736, based on the pathophysiological and molecular results, and 5) determine whether tumor vessels become more efficient, or in other words "normalize", during various schedules of combination therapy.

References:

1. Fenton, B. M., Paoni, S. F., Beauchamp, B. K., and Ding, I. Zonal image analysis of tumour vascular perfusion, hypoxia, and necrosis. Br J Cancer, *86*: 1831-1836, 2002.

2. Kano, M. R., Morishita, Y., Iwata, C., Iwasaka, S., Watabe, T., Ouchi, Y., Miyazono, K., and Miyazawa, K. VEGF-A and FGF-2 synergistically promote neoangiogenesis through enhancement of endogenous PDGF-B-PDGFR{beta} signaling. J Cell Sci., *118*: 3759-3768, 2005.

3. Armulik, A., Abramsson, A., and Betsholtz, C. Endothelial/pericyte interactions. Circ.Res., *97*: 512-523, 2005.

4. McDonald, D. M. and Choyke, P. L. Imaging of angiogenesis: from microscope to clinic. Nat.Med., *9*: 713-725, 2003.

Appendices:

Copy of one abstract (to be presented at the Radiation Research Meeting in Denver on October 17, 2005)

Pathophysiological effects of antibodies to IGF-1R and VEGFR-2 plus fractionated radiation in DU145 prostate carcinoma xenografts. Bruce M Fenton and Scott F Paoni University of Rochester Medical Center, Rochester, New York 14642

Introduction: Several recent reports have demonstrated that the specific scheduling of antiangiogenic strategies with conventional therapy (chemotherapy or radiotherapy) can be critical to ultimate therapeutic response. Our previous studies have shown that alternative antiangiogenic strategies can produce quite opposite effects on tumor oxygenation and blood flow in murine mammary tumors. DC101 (ImClone Systems Inc.), an antiangiogenic monoclonal antibody against vascular endothelial growth factor receptor-2, resulted in substantial tumor hypoxia, while endostatin instead improved tumor oxygenation. The current experiments were designed to determine the pathophysiological effects of both single and combined treatments, using either antiangiogenic strategies or fractionated radiotherapy. AG-013736

Methods: DU145 human prostate xenograft tumors in mice were treated with either: a) saline, b) DC101, c) 15 x 2 Gy daily radiation fractions, d) A12 (ImClone Systems Inc.), an antibody to insulin growth factor receptor-1, or e) the combination of A12 and DC101. Tumor volumes were measured 3 times weekly for 3 wks. Using automated image processing techniques combined with immunohistochemical staining, total and perfused blood vessels were quantified, and tumor hypoxia was estimated by EF5 hypoxia marker uptake.

Results: In comparison to controls, all treatment regimens produced substantial growth delay, with maximal response following the DC101 and the DC101/A12. Total and perfused vessel counts decreased significantly following both DC101 and the DC101/A12 combination, while overall tumor hypoxia increased only for the combination.

Conclusions: In view of the reduced blood flow and/or increased hypoxia following DC101 and the DC101/A12 combination, radiotherapy would be predicted to be more effective when administered prior to the initiation of the antiangiogenic therapy. Ongoing studies are comparing the effects of alternative scheduling (antiangiogenics given pre-, post-, or concurrently with fractionated radiation) to gauge the importance of the accompanying pathophysiological alterations in potentiating combined treatment response.